

The Nature of the Thermal Decomposition of a Catalytically Active Anionic Clay Mineral

W. T. REICHLER,¹ S. Y. KANG, AND D. S. EVERHARDT

Union Carbide Corporation, Specialty Chemicals Division, Technical Center, P.O. Box 670, Bound Brook, New Jersey 08805

Received May 3, 1985

Certain synthetic, anionic clays, after a carefully controlled heat activation, have been shown to promote a wide variety of base catalyzed reactions such as aldol condensations, oxirane polymerizations, carbon-bound H-D exchange, and lactone polymerizations. The changes which take place during the heat activation of such a synthetic, anionic clay mineral, hydrotalcite ($Mg_6Al_2(OH)_{16}(CO_3) \cdot 4H_2O$), have been studied by ^{27}Al nuclear magnetic resonance–magic angle spinning, Auger and XPS spectroscopy, transmission electron microscopy, and high resolution nitrogen desorption techniques. The heating of this material (to $\sim 450^\circ C$) results in the loss of interstitial water, carbon dioxide, and dehydroxylation until a catalytically active material analyzing approximately as $Mg_6Al_2O_8(OH)_2$ remains. This heating does not cause a change in the crystal morphology nor in exfoliation of the layered structure. Instead, numerous fine pores (20–40 Å radius) form perpendicular to the crystal surface from which the gases vent. This is accompanied by an increase in the surface area from about 120 to about 230 m^2/g (N_2 /BET) and a doubling of the pore volume (0.6 to 1.0 cm^3/g , Hg intrusion). The bulk aluminum changes from all octahedral to about 20% tetrahedral–80% octahedral. Auger spectroscopy did not appear to indicate changes in the surface aluminum environment. The X-ray powder pattern changes from that of a diffuse hydrotalcite to a very poor magnesium oxide pattern.

INTRODUCTION

The preparation of catalysts frequently involves heating ("roasting") of a precipitate or an impregnated support. In recent years it has become possible to probe the detailed changes which take place during these procedures. This report discusses the various changes which occur when a particular anionic clay mineral (hydrotalcite $Mg_6Al_2(OH)_{16}(CO_3) \cdot 4H_2O$) is heated in order to render it catalytically active. These heated clays have been found to be catalysts for base catalyzed reactions such as aldol reactions (1, 2), olefin isomerizations, H-D exchange on certain hydrocarbons (2), propylene oxide (3), and β -propiolactone (4) polymerizations.

The structure of hydrotalcite [$Mg_6Al_2(OH)_{16}(CO_3^{2-}) \cdot 4H_2O$] consists of brucite-

like, positively charged layers of magnesium and aluminum hydroxide octahedra sharing edges and has interstitial carbonate anions to charge compensate. Water molecules are also between the metal hydroxide layers (5). The thermal decomposition of this mineral has previously been studied by Miyata (6, 7), and Rouxhet and Taylor (8). Below $200^\circ C$, only interstitial water was lost reversibly; between 250 and $450^\circ C$ both carbon dioxide and further water from the dehydroxylation were lost. This reaction was also reversible, provided the upper temperature did not exceed 550 – $600^\circ C$. It was also found that there was only a modest expansion of the surface area and that both acidic and basic centers had formed on heating (7).

In this investigation it was of particular interest to discover what changes in the crystal morphology, the metal coordination number, and the bulk and surface composi-

¹ To whom correspondence should be addressed.

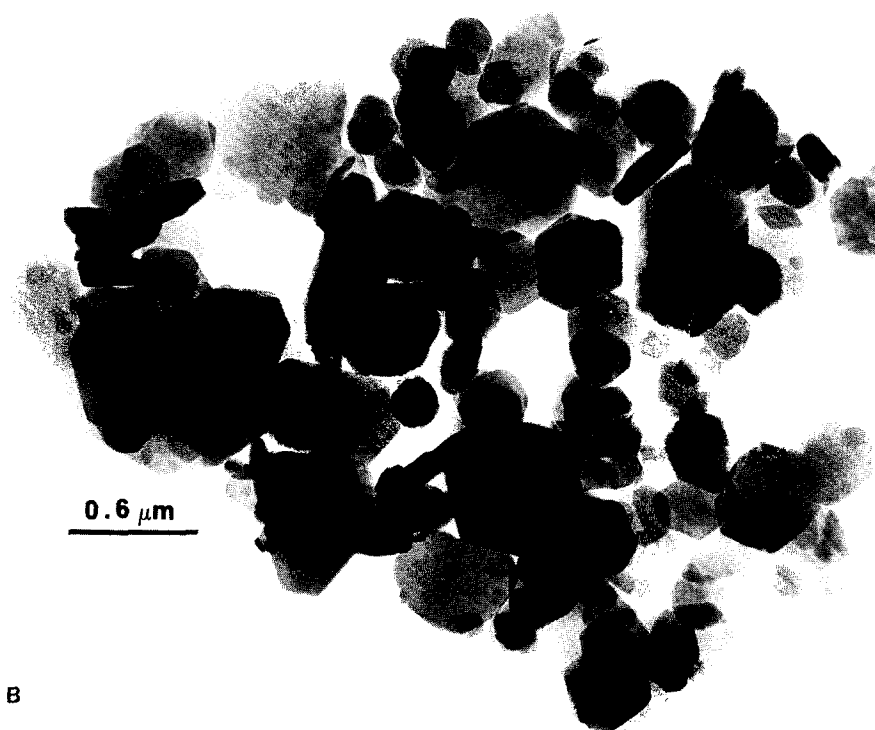
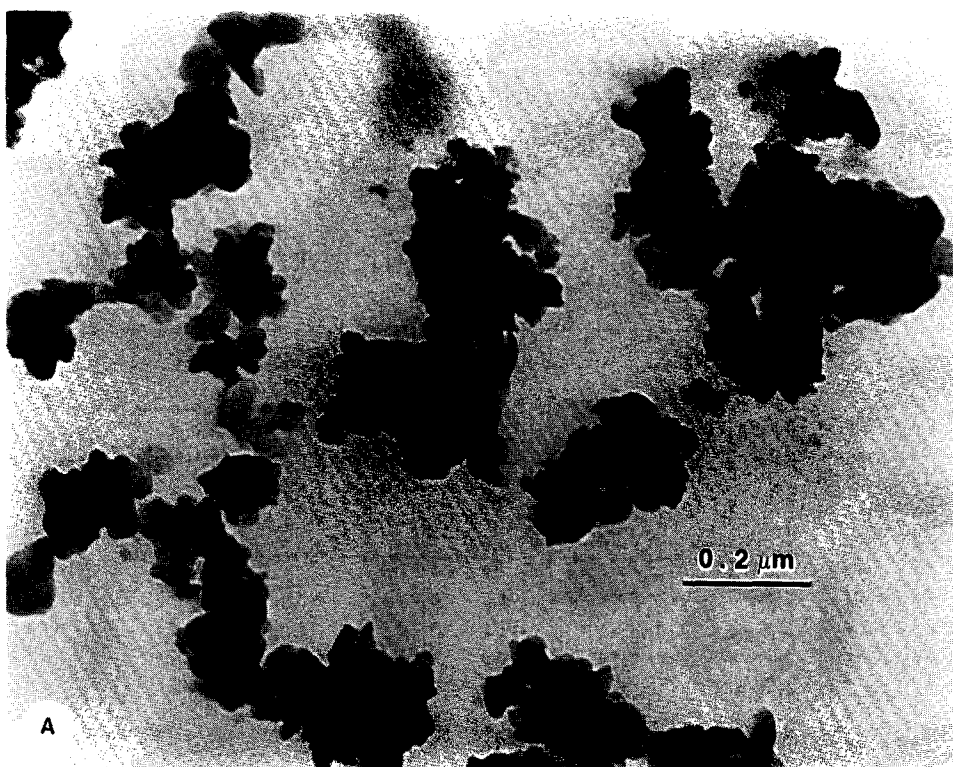


FIG. 1. Transmission electron micrograph of hydrotalcite. (A) 65°C crystallized, (B) 200°C crystallized.

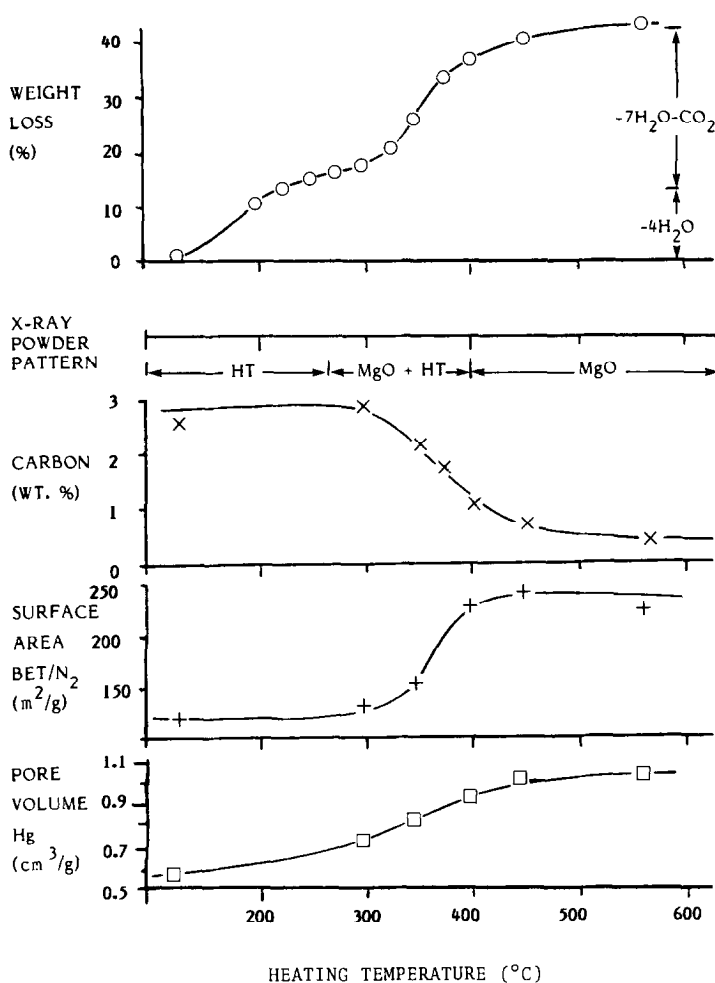


FIG. 2. Changes in properties on thermal decomposition of hydrotalcite (65°C/18 hr crystallized).

tion had taken place on heating synthetic hydrotalcite.

EXPERIMENTAL

Preparation of Mg-Al-CO₃ hydrotalcite.

A solution of 256 g $\text{Mg}(\text{NO}_3)_2 \cdot 6\text{H}_2\text{O}$ (1.00 mole) and 187.5 g $\text{Al}(\text{NO}_3)_3 \cdot 9\text{H}_2\text{O}$ (0.50 mole) in 700 ml distilled water was added to a solution of 280 g, 50% aq. NaOH (3.50 moles), 100 g Na_2CO_3 (anhydr. 0.943 mole) in 1000 ml distilled water. The addition took about 4 hr and was carried out with vigorous agitation at or below 35°C. Following the addition, which resulted in a heavy slurry, the flask contents were heated at 65 ± 5°C for about 18 hr with good mixing.

The slurry was then cooled to room temperature, filtered, and washed until the sodium content of the resulting solid was below 0.1% (dry basis). The solid was dried (125°C/vacuum/18 hr) resulting in 100–120 g of a white powder. The X-ray powder pattern of this is that of hydrotalcite; the peaks are relatively broad due to the small crystal size. Anal. found: ash, 57.39; Mg, 35.34; Al, 17.72; Na, 0.006; N, 0.012; C, 2.50. Calculated for $\text{Mg}_6\text{Al}_{2.28}(\text{OH})_{16.56}(\text{CO}_3^{2-})_{1.14} \cdot 6\text{H}_2\text{O}$; ash, 58.38; Mg, 38.51; Al, 16.26; C, 2.11 (Mg and Al on ashed basis). The crystal size and perfection depend upon the time and temperature of crystallization. Thus, at 65°C/18 hr very imperfect laminar

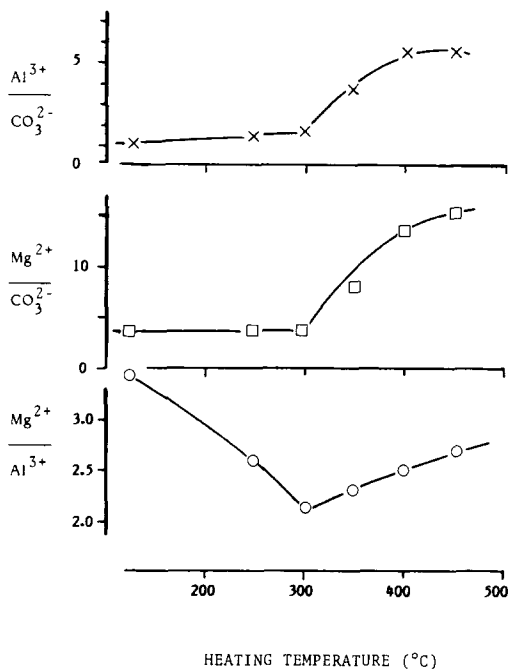


FIG. 3. Changes in surface composition during thermal decomposition of hydrotalcite (65°C/18 hr crystallized) (atom/mole%).

particles were obtained (transmission electron micrograph TEM, Fig. 1A); at 200°C/18 hr (under pressure) well developed hexagonal crystals were produced (Fig. 1B).

Heat treatment of hydrotalcite. One-gram samples of the 65°C/18 hr crystallized hydrotalcite were heated in air at the required temperature for 12–18 hr in a small muffle furnace. Total carbon was determined by combustion/adsorption. The BET surface areas were determined by standard, multipoint techniques; mercury intrusion was used for the pore volume determinations.

DISCUSSION

Figure 2 illustrates some of the changes which take place on heating to 450–500°C. The weight loss of the hydrotalcite (65°C/18 hr crystallization time) takes place in two stages, as found by others (7, 8). Interstitial water is lost up to 300°C, followed by the loss of water due to dehydroxylation as well as of carbon dioxide (carbon analyses,

Fig. 2). X-Ray photoelectron spectroscopy (XPS) shows a pronounced decrease in surface carbonate between 300 and 350°C (Fig. 3; XPS readily distinguishes CO_3^{2-} from typical surface hydrocarbon). By 550°C, no CO_3^{2-} is detected by XPS on the surface of the hydrotalcite decomposition product. The reason(s) for the fairly large changes in the surface Mg/Al ratio is not clear. The decrease in this ratio on heating to 300°C followed by a modest rise above this temperature suggests that some form of reorganization of the surface is taking place which involves not only the magnesium and aluminum ions, but also the loss of interstitial water followed by dehydroxylation-carbon dioxide expulsion. The surface area and pore volume both increased (Fig. 2), the former from about 120 to 220 m^2/g after heating, the pore volume from 0.6 to 1.0 cm^3/g . Similarly, the surface area of a hydrotalcite crystallized at 200°C/18 hr increased from 13.9 to 19.4 m^2/g on heating to 450°C (not shown in Fig. 2). A calculation based on the geometry of Fig. 1B crystals results in a 12 m^2/g external surface area (vs 13.9 m^2/g measured). This demonstrates that there is little internal surface area in these crystals. The decomposition of hydrotalcite could involve a delamination of the individual layers of metal oxide octahedra, very similar to the exfoliation of vermiculite or a mechanical peeling apart of mica crystals. An extensive delamination of this structure should raise the measured surface area by a factor of 5–10, far more than the observed increase. The TEM of the hydrotalcite (200°C/18 hr crystallized) heated to 450° (Fig. 4) shows that the particle morphology has been retained and an edge-on view (not shown) shows no increase in crystal thickness. Therefore, delamination cannot be a mechanism for the hydrotalcite decomposition. A closer examination of Fig. 4 shows that the crystal surfaces are pock-marked and cratered, as compared to the smooth surface of the unheated hydrotalcite (Fig. 1B). This suggests that the exiting steam and

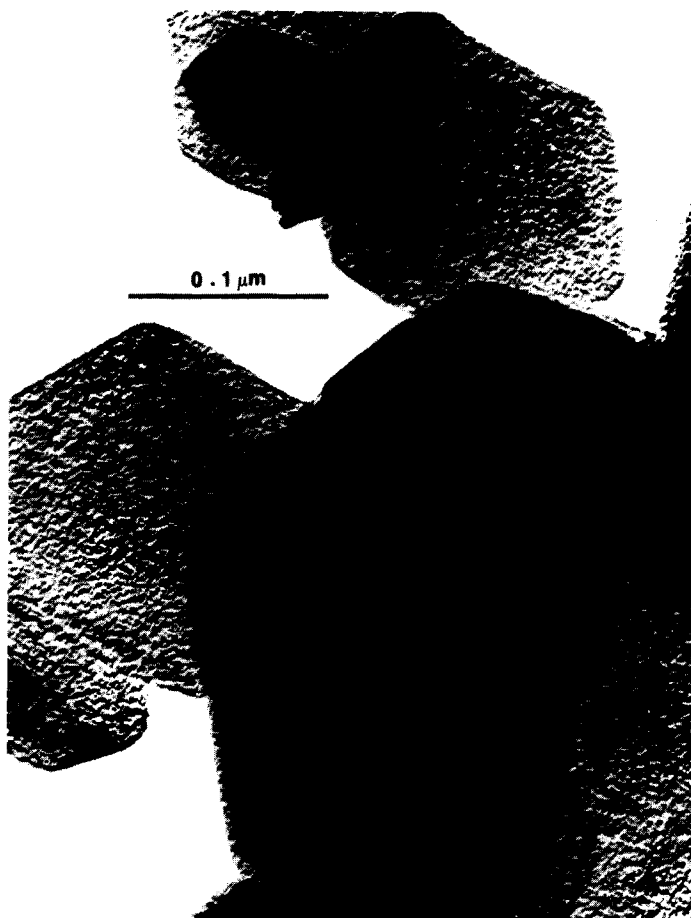


FIG. 4. TEM of hydrotalcite (200°C/18 hr crystallized + 450°C heated).

carbon dioxide escaped through holes in the crystal surface which then appear as small, fairly regularly spaced craters. This

escape mechanism explains the relatively small increase in the surface area on heating. It appears that the interlaminar forces in hydrotalcite are sufficiently strong, even during heating, so that interstitial venting is not possible.

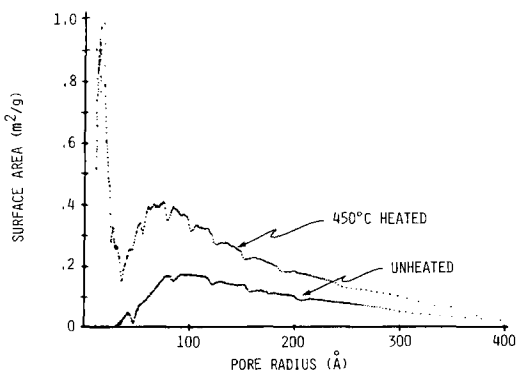


FIG. 5. Pore surface area (m^2/g) vs pore radius (\AA) (hydrotalcite 65°C/18 hr crystallized).

This cratering theory is further supported by nitrogen pore volume measurements and surface areas calculated from this data (N_2 desorption isotherms). Figure 5 is a plot of the unheated hydrotalcite pore surface area against pore radius (of 65°C/18 hr crystallized hydrotalcite) and is compared with the same hydrotalcite sample after heating to 450°C/18 hr. The former shows only a broad range of pores in the range 75–300 \AA . The heated sample adds to this numerous pores in the region 20–40 \AA . Clearly, heating has resulted in numerous fine pores

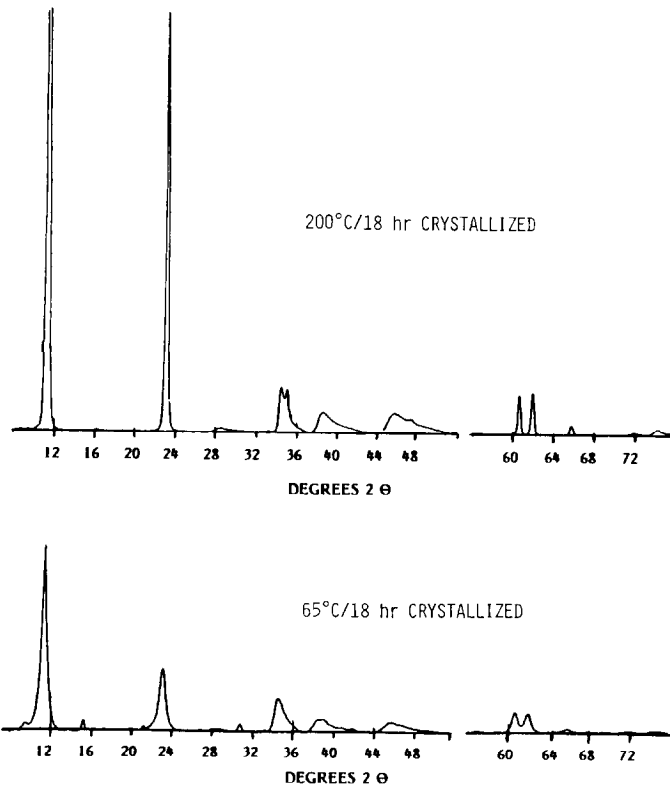


FIG. 6. X-Ray powder patterns of hydrotalcites 200°C/18 hr crystallized.

which collectively constitute about 60% of the surface area.

In Fig. 6 are the X-ray powder patterns of 65°C/18 hr and 200°C/18 hr crystallized hy-

drotalcites. The high temperature preparation yields a product which has intense and very sharp diffractions while the 65°C crystallized material has a relatively broad and

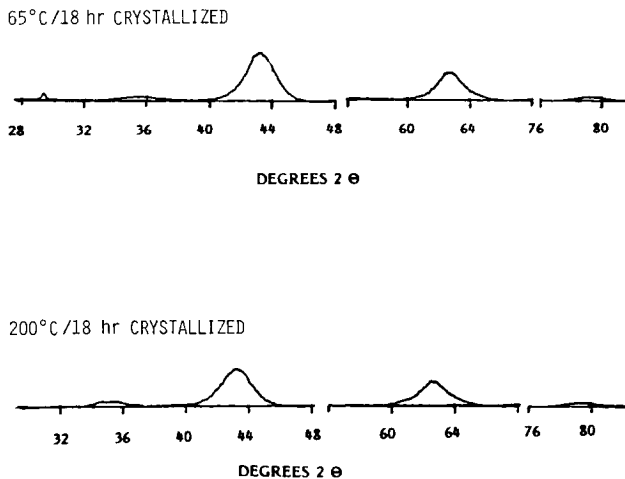


FIG. 7. X-Ray powder patterns of heated (450°C) hydrotalcites.

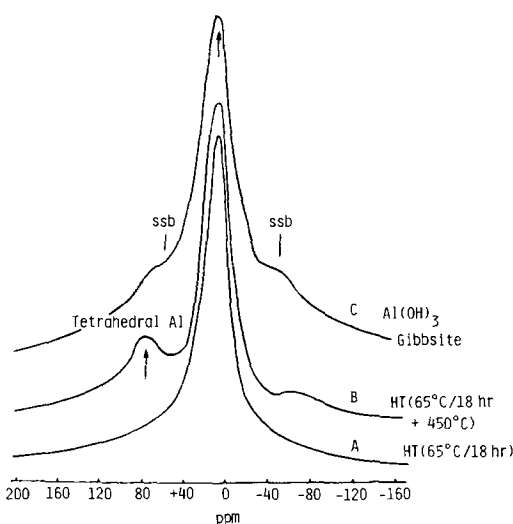


Fig. 8. ^{27}Al mass-NMR spectrum of (A) hydrotalcite ($65^\circ\text{C}/18$ hr crystallized), (B) hydrotalcite ($65^\circ\text{C}/18$ hr crystallized + 450°C heated), (C) gibbsite $\text{Al}(\text{OH})_3$.

diffuse pattern. On heating to 450°C (Fig. 7) both yield products which have very broad, diffuse, and weak diffractions of magnesium oxide.

Solid state ^{27}Al -NMR MAS (nuclear magnetic resonance-magic angle spinning) spectroscopy was also used to examine the nature of the hydrotalcite decomposition product (450°C heated). Figure 8A is the spectrum of the hydrotalcite crystallized at $65^\circ\text{C}/18$ hr (unheated) and shows, as expected, a single resonance (+10 ppm) due to octahedral aluminum. After the sample was heated to 450°C , a shoulder developed (Fig. 8B) at +75 ppm which is due to tetrahedral aluminum (9, 10). The third spectrum is that of gibbsite [$\text{Al}(\text{OH})_3$], which is exclusively octahedral aluminum hydroxide (Fig. 8C). The tetrahedral aluminum content of a hydrotalcite ($65^\circ\text{C}/18$ hr crystallized) thermally decomposed at 450°C is thought to be less than 20%. Accurate quantification of the tetrahedral aluminum content by NMR was complicated by the presence of fairly intense spinning side bands (ssb); however, the presence of low concentrations of T_d aluminum is confirmed by NMR. Since this is a bulk measurement,

an attempt was made to examine the coordination of the surface aluminum by measuring the modified Auger parameter of aluminum using XPS.

Recent work of Wagner and co-workers (11) has demonstrated that the modified aluminum Auger parameter, α'_{Al} , can distinguish aluminum in O_h and T_d environments ($\alpha' = EK_{\text{Auger}} - KE_{\text{photoelectron}} + E_{\text{source energy}}$). Table 1 summarizes the results for unheated and heated hydrotalcite and some selected reference compounds. The α'_{Al} values for the unheated and the heated hydrotalcite samples do not differ appreciably from each other nor are they in concordance with the α'_{Al} values of octahedral or tetrahedral models of known structures. This may be due to the fact that the results of Wagner (11) are from aluminum silicates and aluminum oxides and hydroxide which are inappropriate reference compounds. The true effects of Mg^{2+} on the α' of aluminum are not known at this time.

In summary, hydrotalcite on heating (450°C) appears to lose its water and carbon

TABLE I
Aluminum XPS and Auger Parameter Data

Sample	Al_2p	α'_{Al}	Reference
Octahedrally coordinated aluminum			
$\alpha\text{-Al}_2\text{O}_3$	73.85	1462.09	(11)
$\alpha\text{-Al}_2\text{O}_3$	73.72	1461.55	(11)
$\text{Al}(\text{OH})_3$ gibbsite	74.00	1461.43	(11)
$\text{Al}(\text{OH})_3$ gibbsite	74.3	1461.3	This work
60°C crystallized hydrotalcite	74.2	1460.6	This work
200°C crystallized hydrotalcite	74.0	1460.9	This work
Tetrahedrally coordinated aluminum			
Na-A zeolite	73.6	1460.53	(11)
Albite	74.34	1460.81	(11)
Natrolite	74.25	1460.78	(11)
Na-X zeolite	74.13	1460.38	(11)
60°C crystallized and 450°C heated hydrotalcite	73.7	1461.0	This work
200°C crystallized and 450°C heated hydrotalcite	73.4	1461.0	This work

dioxide by a cratering mechanism (vent holes in the crystal surface) rather than by exfoliation of the metal oxide layers. This is in line with only a modest increase in surface area, a retention of the crystal morphology, the appearance of pockmarks on the crystal surface, and numerous fine pores which are in the range 20–40 Å. Spectroscopic techniques show that only a small portion of the total aluminum is converted to a tetrahedral metal oxide, possibly residing on the surface.

ACKNOWLEDGMENTS

The authors thank the personnel of Union Carbide Corporation's Central Scientific Laboratory, Tarrytown, New York, who aided in the characterization of these materials. The N₂ surface area and pore volumes were determined by Omicron Technology Corporation, Berkeley Heights, New Jersey. The elemental analyses were made by Galbraith Laboratories, Knoxville, Tennessee.

REFERENCES

1. Reichle, W. T., *J. Catal.* **94**, 547 (1985).
2. Reichle, W. T., U.S. 4,458,026 (To Union Carbide Corp., July 3, 1984).
3. Kohjiya, S., Sato, T., Nakayama, T., and Yamashita, S., *Makromol. Chem., Rapid Commun.* **2**, 231 (1981).
4. Nakatsuka, T., Kawasaki, H., Yamashita, S., and Kohjiya, S., *Bull. Chem. Soc. Jap.* **52**, 2449 (1979).
5. Allmann, R., and Jepson, H. P., *Neues Jahrb. Mineral. Monatsh.*, 544 (1969).
6. Miyata, S., *Clays Clay Miner.* **23**, 369 (1975).
7. Miyata, S., Kumara, T., Hattori, H., and Tanabe, K., *Nippon Kayaku Zasshi* **92**, 514 (1971).
8. Rouxhet, P. G., and Taylor, H. F. W., *Chimia* **23**, 480 (1969).
9. John, C. S., Alma, N. C. M., and Hays, G. R., *Appl. Catal.* **6**, 341 (1983).
10. Thomas, J. M., Kinowski, J., Wright, P. A., and Roy, R., *Angew. Chem., Int. Ed. Engl.* **22**, 614 (1983).
11. Wagner, C. D., Passoja, D. E., Hillery, H. F., Kinisky, T. G., Six, H. A., Jansen, W. T., and Taylor, J. A., *J. Vac. Sci. Technol.* **21**, 933 (1982).